Formation and Stability of Size-, Shape-, and Structure-Controlled CdTe Nanocrystals: Ligand Effects on Monomers and Nanocrystals

W. William Yu, Y. Andrew Wang, and Xiaogang Peng*

Department of Chemistry & Biochemistry, University of Arkansas, Fayetteville, Arkansas 72701

Received August 5, 2003

The formation of nearly monodisperse CdTe nanocrystals—dots (either zinc blende or wurtzite crystal structure), rods, and tetrapods—in a noncoordinating solvent was studied. Several strong ligand effects were observed, and the ligand effects on the monomers were found to play a more important role than the ligand effects on the nanocrystals. Experimental results suggest that, instead of monomer concentrations, monomer activities is a more relevant term for understanding the formation of nanocrystals because strong ligands always exist in the reaction solutions. The bonding strength and the steric effects of ligands dramatically affect the reactivity of monomers and are considered as contributors to the activity coefficients of monomers. The overall optical properties of the as-prepared CdTe nanocrystals are better than those reported in the literature and comparable to the standard CdSe nanocrystal system. The configuration of the hydrocarbon chains of the ligands on the surface of each nanocrystal also plays a critical role in determining the stability of CdTe nanocrystals.

Introduction

The first key issue for fundamental studies and technical applications of colloidal semiconductor nanocrystals is the synthesis of high-quality nanocrystals. This has recently advanced significantly due to the introduction of the organometallic approaches in the early 90s[1,2] and, after 2000, the alternative approaches.[3−5] With all of these progressions, CdSe nanocrystals became the best system in terms of the overall control of the size,[2,4,6,7] shape,[8−10] size/shape distribution, and optical quality.[11] These developments have benefited greatly from the related mechanism studies, especially the introduction and advancement of the alternative routes.[6,9,10,12]

The chemical nature and physical dimension of the ligands for nanocrystals have been widely noticed to act as an important factor during the formation of nanocrystals. For example, selective binding on the surface of nanocrystals, or the ligand template effect, has been widely suggested to control the shape of nanocrystals.[9,13−25] However, any ligands added to a synthetic system are not only the ligands for the resulting nanocrystals but also the ligands for the monomers. It is possible that, in the growth stage, the ligands may influence the monomers and nanocrystals simultaneously. However, in the initial stage of crystallization, the nucleation stage, ligand effects on crystals should not be an important factor. Instead, the properties of the monomers play the determining role. To date, ligand effects on monomers have been mostly ignored in the

* To whom correspondence should be addressed. Phone: 479-575-4612. Fax: 479-575-4049. E-mail: xpeng@comp.uark.edu.

(1) Steigerwald, M. L.; Brus, L. E. *Acc. Chem. Res.* **1990**, *23*, 183−188.
(2) Murray, C. B.; Norris, D. J.; Bawendi, M. G. *J. Am. Chem. Soc.* **1993**, *115*, 8706−8715.
(3) Peng, Z. A.; Peng, X. *J. Am. Chem. Soc.* **2001**, *123*, 183−184.
(4) Qu, L.; Peng, Z. A.; Peng, X. *Nano Lett.* **2001**, *1*, 333−336.
(5) Peng, X. *Chem. Eur. J.* **2002**, *8*, 334−339.
(6) Peng, X.; Wickham, J.; Alivisatos, A. P. *J. Am. Chem. Soc.* **1998**, *120*, 5343−5344.
(7) Cumberland, S. L.; Hanif, K. M.; Javier, A.; Khitrov, G. A.; Strouse, G. F.; Woessner, S. M.; Yun, C. S. *Chem. Mater.* **2002**, *14*, 1576−1584.
(8) Peng, X.; Manna, L.; Yang, W. D.; Wickham, J.; Scher, E.; Kadavanich, A.; Alivisatos, A. P. *Nature* **2000**, *404*, 59−61.
(9) Manna, L.; Scher, E. C.; Alivisatos, A. P. *J. Am. Chem. Soc.* **2000**, *122*, 12700−12706.
(10) Peng, Z. A.; Peng, X. *J. Am. Chem. Soc.* **2002**, *124*, 3343−3353.
(11) Qu, L.; Peng, X. *J. Am. Chem. Soc.* **2002**, *124*, 2049−2055.
(12) Peng, Z. A.; Peng, X. G. *J. Am. Chem. Soc.* **2001**, *123*, 1389−1395.
(13) Ahmadi, T. S.; Wang, Z. L.; Green, T. C.; Henglein, A.; El-Sayed, M. A. *Science* **1996**, *272*, 1924−1926.
(14) Petroski, J. M.; Wang, Z. L.; Green, T. C.; El-Sayed, M. *J. Phys. Chem. B* **1998**, *102*, 3316−3320.
(15) Chang, S. S.; Shih, C. W.; Chen, C. D.; Lai, W. C.; Wang, C. R. C. *Langmuir* **1999**, *15*, 701−709.
(16) Pileni, M. P. *Adv. Mater.* **1999**, *10*, 1358−1362.
(17) Li, Y.; Liao, H.; Ding, Y.; Fan, Y.; Zhang, Y.; Qian, Y. *Inorg. Chem.* **1999**, *38*, 1382−1387.
(18) Bradley, J. S.; Tesche, B.; Busser, W.; Maase, M.; Reetz, M. T. *J. Am. Chem. Soc.* **2000**, *122*, 4631−4636.
(19) Puntes, V. F.; Krishnan, K. M.; Alivisatos, A. P. *Science* **2001**, *291*, 2115−2117.
(20) Jun, Y.-w.; Lee, S.-M.; Kang, N.-J.; Cheon, J. *J. Am. Chem. Soc.* **2001**, *123*, 5150−5151.
(21) Soulantica, K.; Maisonnat, A.; Fromen, M. C.; Casanove, M. J.; Lecante, P.; Chaudret, B. *Angew. Chem., Int. Ed.* **2001**, *40*, 2984−2986.
(22) Yang, Q.; Tang, K.; Wang, C.; Qian, Y.; Zhang, S. *J. Phys. Chem. B* **2002**, *106*, 9227−9230.
(23) Lee, S.-M.; Jun, Y.-w.; Cho, S.-N.; Cheon, J. *J. Am. Chem. Soc.* **2002**, *124*, 11244−11245.
(24) Kim, Y.-H.; Jun, Y.-w.; Jun, B.-H.; Lee, S.-M.; Cheon, J. *J. Am. Chem. Soc.* **2002**, *124*, 13656−13657.
(25) Lee, S.-M.; Cho, S.-N.; Cheon, J. *Adv. Mater.* **2003**, *15*, 441−444.

10.1021/cm034729t CCC: $25.00
Published on Web 10/03/2003

growth of both nanocrystals and bulk-sized crystals. This may hinder the establishment of a complete picture for understanding the formation of high-quality nanocrystals as well as crystallization in general.

Ligand effects on monomers became more important after the introduction of noncoordinating solvents for the synthesis of high-quality semiconductor nanocrystals.[26] Preliminary results revealed that the monomer reactivity in noncoordinating solvents can be fine-tuned by varying the ligand concentration and chain length.[26,27] With the tunable reactivity of the monomers, a balanced nucleation and growth became possible, which is the key for the control of size and size distribution during the synthesis of nearly monodisperse dot-shaped nanocrystals.[26,27] The results described below are about high-quality CdTe nanocrystals. These results reveal that, in addition to improving the control of the size and size distribution of dot-shaped nanocrystals, ligand effects play a critical role in the control of shape, shape distribution, crystal structure, and stability of the nanocrystals. Instead of monomer concentration, the results of this report indicate that monomer activity—"effective monomer concentration"—would be a more relevant term. The activity coefficient accounts for the bonding strength of the anchoring group and the steric effects of the periphery of ligands.

We chose CdTe nanocrystals grown in noncoordinating organic solvents as our system. CdTe nanocrystals could potentially compete with CdSe nanocrystals in many applications if their overall quality could be as high as CdSe nanocrystals because its emission color window can be at least as broad as CdSe nanocrystals. In fact, for certain applications, such as solar cells[28] and in vivo biomedical detections,[29,30] CdTe nanocrystals are potentially better candidates because of their additional near-IR activities in comparison to CdSe nanocrystals. Before this report, it was possible to obtain dot-shaped CdTe nanocrystals of high quality in a relatively small size range (with the first absorption peak between 600 and 680 nm) and reasonable quality rods with some control over the aspect ratio through the alternative approaches in coordinating solvents.[3] Dot-shaped CdTe nanocrystals with relatively broad size distributions can also be synthesized using traditional organometallic approaches[31,32] and aqueous solution approaches.[33] Typically, the aqueous solution approaches generate particles with relatively small sizes and large particles are the products in organic media.

The results described below demonstrate that the overall control of the size, shape, crystal structure, and optical properties of CdTe nanocrystals can be promoted to a level similar to, or better than, the standard CdSe nanocrystal system by taking advantage of the ligand effects in noncoordinating solvents.

Experimental Section

Chemicals. CdO (99.99+%), Te powder (200 mesh, 99.8%), tributylphosphine (TBP) (97%), trihexylphosphine (THP) (98%), trioctylphosphine (TOP) (97%), oleic acid (OA) (90%), eladic acid (EA) (98%), 1-octadecene (ODE) (tech. 90%, the other 10% are various isomers of ODE and *n*-octadecane), $CDCl_3$ (99.9%), and 10% HCl−D_2O were purchased from Aldrich; stearic acid (SA) (99%) was obtained from Avocado; tetradecylphosphonic acid (TDPA) (98%) and octadecylphosphonic acid (ODPA) (98%) were from Alfa Aesar. Toluene, chloroform, hexane, and methanol were purchased from EM Science.

Synthesis of CdTe Nanocrystals. Standard procedures were followed for the synthesis of semiconductor nanocrystals at high temperatures.[2,10] The photoluminescence quantum yield (PL QY) of the nanocrystals was measured following the same procedure used previously.[11] Typical synthetic procedures of the CdTe nanocrystals with different shapes or different crystal structures are briefly described below.

Typical Synthesis of Dot-Shaped CdTe Nanocrystals with Wurtzite Structure. A Te injection solution containing 0.0064 g of Te (0.050 mmol) was prepared in a glovebox by dissolving Te powder in 0.0576 g of TBP and then diluted with ODE to 2 g. The Te injection solution was then brought out of the glovebox in a vial sealed with a rubber subseal. A mixture (4 g in total) of CdO (0.0128 g, 0.10 mmol), OA (0.1125 g, 0.40 mmol), and ODE was heated in a three-neck flask to 300 °C to obtain a clear solution. At this temperature, the Te injection solution was quickly injected into the hot solution. The reaction mixture was allowed to cool to 260 °C for the growth of the CdTe nanocrystals. The synthesis was carried out under argon flow. Aliquots were taken at different time intervals, and UV/vis (HP 8453 diode array spectrophotometer) and PL (HITACHI F-2500 fluorescence spectrophotometer) spectra were recorded for each aliquot. Difference was not observed when 99+% oleic acid (Aldrich) was used instead of the 90% reagent. For all optical measurements, the absorbance at the first absorption peak was kept below 0.2.

Typical Synthesis of Dot-Shaped CdTe Nanocrystals with Zinc Blende Structure. The only difference between this synthesis and the one described above was that 0.20 mmol of ODPA (0.0669 g) or 0.20 mmol of TDPA (0.0558 g) was used in place of 0.4 mmol of OA.

Typical Synthesis of CdTe Tetrapods. CdTe nanocrystals with a tetrapod shape can be obtained by following the same procedure described above for nanocrystals with wurtzite structure if TOP is used for the preparation of the Te injection solution, instead of TBP. For this reaction and the synthesis of rod-shaped nanocrystals, OA was used as the ligands to dissolve CdO powder in ODE.

Typical Synthesis of CdTe Rods. CdTe nanocrystals with a rod shape were obtained by using 0.05 mmol of CdO dissolved by 0.2 mmol of OA in ODE and 0.025 mmol of Te dissolved by 0.029 g of TOP. The other reaction conditions were kept the same as those for the formation of tetrapods.

Purification of the Nanocrystals. The purification procedure was published previously,[34] and a brief description is given as follows. The ODE solution of the as-prepared nanocrystals was mixed with an equal volume mixture of hexane and methanol (1/2, v/v) by vigorous shaking and then centrifuged and the ODE phase was extracted. This procedure was repeated once and then the nanocrystals in the ODE phase were precipitated with excess acetone. The precipitate was isolated by centrifugation/decantation and dried under argon at room temperature. The final powder product can be redissolved in a desired solvent (toluene, chloroform, or hexane) for certain measurements. The complete removal of cadmium

(26) Yu, W. W.; Peng, X. *Angew. Chem., Int. Ed.* **2002**, *41*, 2368−2371.
(27) Battaglia, D.; Peng, X. *Nano Lett.* **2002**, *2*, 1027−1030.
(28) Greenham, N. C.; Peng, X. G.; Alivisatos, A. P. *Phys. Rev. B* **1996**, *54*, 17628−17637.
(29) Dubertret, B.; Skourides, P.; Norris, D. J.; Noireaux, V.; Brivanlou, A. H.; Libchaber, A. *Science* **2002**, *298*, 1759−1762.
(30) Wu, X.; Liu, H.; Liu, J.; Haley, K. N.; Treadway, J. A.; Larson, J. P.; Ge, N.; Peale, F.; Bruchez, M. P. *Nat. Biotechnol.* **2003**, *21*, 41−46.
(31) Mikulec, F. V.; Bawendi, M. G. *Mater. Res. Soc. Symp. Proc.* **2000**, *581*, 139−144.
(32) Talapin, D. V.; Haubold, S.; Rogach, A. L.; Kornowski, A.; Haase, M.; Weller, H. *J. Phys. Chem. B* **2001**, *105*, 2260−2263.
(33) Gaponik, N.; Talapin, D. V.; Rogach, A. L.; Hoppe, K.; Shevchenko, E. V.; Kornowski, A.; Eychmueller, A.; Weller, H. *J. Phys. Chem. B* **2002**, *106*, 7177−7185.
(34) Yu, W. W.; Qu, L.; Guo, W.; Peng, X. *Chem. Mater.* **2003**, *15*, 2854−2860.

precursors from the final solution was confirmed by UV−vis spectroscopy.

Cd Monomer Concentrations. Cd monomer concentrations were measured on a GBC 932 plus atomic absorption spectrophotometer. About 1 mL of toluene was placed into a clean vial; the vial was then sealed with rubber septa and weighed as M_1. An aliquot at a given reaction time was taken out from the reaction flask with a small syringe and quickly transferred into a vial with toluene. The rapid cooling of the hot aliquot by the cold toluene sufficiently quenched the growth of the nanocrystals. The total weight was measured as M_2. The weight of the aliquot was calculated as $M_2 - M_1$. The solution of each aliquot was purified as stated above, and all extraction solutions containing either the unconverted Cd monomers or the purified nanocrystals were collected in two separate vials. The solvent in the collected solutions was completely evaporated at 50 °C and the solid residuals in both vials were digested by several drops of 1:3 (v/v) HCl/HNO_3 separately and then diluted by pure water to certain concentrations of Cd. The Cd concentrations of both diluted solutions were measured by atomic absorption (AA). With the known dilution factors, the concentrations measured by AA were used for the calculations of the Cd monomer concentration in the reaction flask at the given moment when the aliquot was taken. The results were well-matched based on either the unconverted Cd monomers or the Cd monomers in the form of nanocrystals.

TEM. TEM (JEOL 100CX) specimen were prepared by dipping a Formvar-coated copper grid into a toluene solution of the aliquot, and the grid with the nanocrystals was dried in air. The acceleration voltage used was either 80 or 100 kV. The average sizes of the CdTe nanocrystals from more than 10 samples were calculated by measuring 400−500 isolated nanocrystals in a given area of a TEM image. These data points were plotted as a TEM-absorption peak sizing curve (see Supporting Information) and were used to determine the average size of a sample by its first absorption peak position.

^{1}H NMR. ^{1}H NMR analysis (JEOL 270 MHz) was carried out by using either commercially available chemicals or the recovered ligands (OA, EA, SA) dissolved in $CDCl_3$. To obtain the recovered ligands, purified nanocrystal samples were first digested by a HCl−D_2O solution, and then the organic ligands were extracted by $CDCl_3$ from the D_2O solution.

IR. IR (Nicolet Impact 410) spectra of CdTe nanocrystals, OA, EA, SA, $Cd(OA)_2$, $Cd(EA)_2$, and $Cd(SA)_2$, were obtained by mixing a given sample in a KBr pellet. $Cd(OA)_2$, $Cd(EA)_2$, and $Cd(SA)_2$ were synthesized by reacting excess acids with CdO. Briefly, 1.00 mmol of CdO (0.128 g), 2.1 mmol of fatty acid (0.593 g of OA, 0.593 g of EA, or 0.597 g of SA), and 6.00 g of ODE were mixed together and heated to 180 °C under argon flow for 4−5 min to obtain a colorless solution. After that, the solution was allowed to cool to room temperature, and a white precipitate was obtained by decanting the liquid portion. The solid white precipitate was washed with warm toluene (50−60 °C) several times and then dried under argon to give a white solid powder of pure $Cd(EA)_2$ or $Cd(SA)_2$. Different from the other two salts, $Cd(OA)_2$ could only be obtained as a waxlike substance.

XRD Patterns. XRD patterns were obtained by the standard powder diffraction methods with a Philips PW1830 X-ray powder diffractometer using a Cu Kα line. Purified powder CdTe nanocrystals were crushed into fine powder for the XRD analysis.

Results

Size Range of Dot-Shaped CdTe Nanocrystals. The size range of dot-shaped CdTe nanocrystals grown in ODE as the noncoordinating solvent, which covers the sum of all of the aqueous approaches[33] and the coordinating solvent approaches,[3,31,32] was approximately between 2 and 11 nm. The emissions of very small and very big CdTe nanocrystals were very weak.

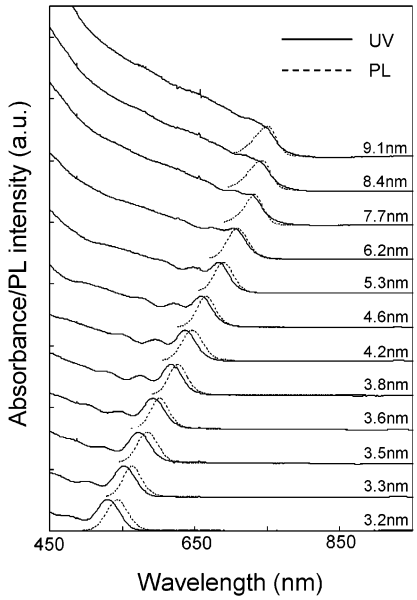

Figure 1. UV−vis and PL spectra of as-prepared CdTe dots.

The corresponding PL peak position for the CdTe nanocrystals with reasonable emission brightness is between 530 and 760 nm (Figure 1). Without any size sorting, all UV−vis and PL spectra of the as-prepared CdTe nanocrystals shown in Figure 1 are at least comparable to the best optical spectra of CdTe dots, which were obtained through alternative approaches in coordinating solvents.[3] Typical PL fwhm of those as-prepared samples is in the range between 27 and 34 nm. Nanocrystals in this size range with the optical properties shown in Figure 1 can be reproducibly synthesized. Sizes of CdTe nanocrystals were varied by varying the ligand concentration, the nature of the ligands, and the structure of the ligands. Secondary injections were also used for the controlled growth of the large size nanocrystals (see Supporting Information). TEM images of several representative dot-shaped nanocrystals can be found in Figure 2 and in the Supporting Information.

Shape and Shape Distribution. Shape and shape distribution of CdTe nanocrystals grown in ODE were controlled by varying the ligands and the initial monomer concentrations. In fact, the shape control of the elongated nanocrystals shown in Figure 2 is significantly better than that for CdSe nanocrystals reported in the literature.[8−10] Elongated CdTe nanocrystals have previously been synthesized using CdO as the cadmium precursor in coordinating solvents.[3] However, the purity of the shapes and the aspect ratio of the elongated nanocrystals were not well-controlled.

The general trend observed in the formation of elongated CdSe nanocrystals in coordinating solvents of which high monomer concentrations yield elongated nanocrystals[10,12] was observed again in the case of CdTe nanocrystals grown in ODE. However, the growth of elongated CdTe nanocrystals revealed a more sophisticated chemistry for shape control. As shown in Figure 2, in addition to the initial monomer concentration, the nature and chain length of ligands in the system played a critical role.

CdTe nanocrystals synthesized using phosphonic acids, either ODPA or TDPA, were all dot shapes within

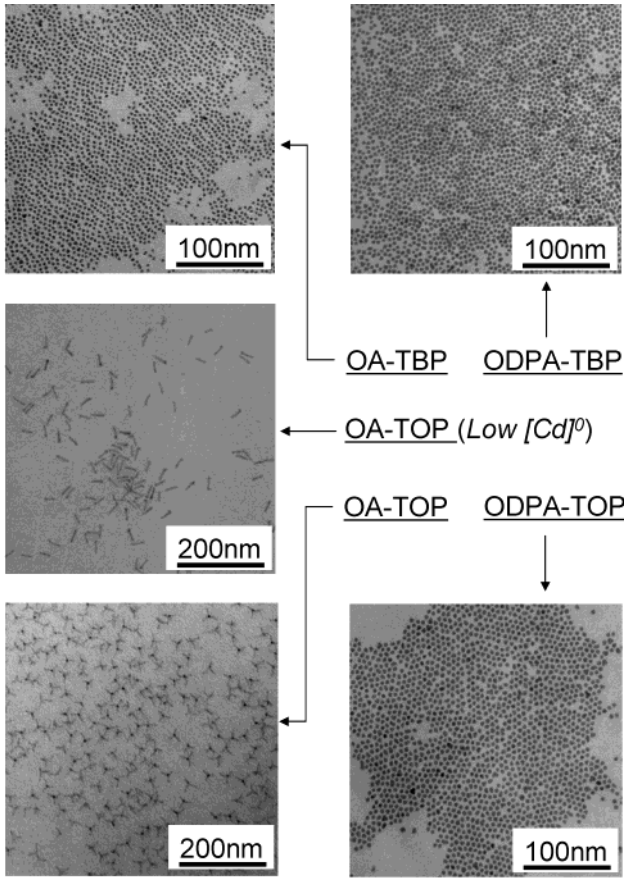

Figure 2. Shape control of as-prepared CdTe nanocrystals by varying the nature and chain length of ligands. Note: All reactions were carried out under identical conditions except the initial Cd concentration ($[Cd]^0$) for the middle case (OA−TOP).

the entire range of the initial cadmium monomer concentration ($[Cd]^0$) tested, even if the chain length of the phosphine was varied (see representative TEM pictures shown on the right panel in Figure 2). On the other hand, as reported previously, if the synthesis was performed in a TOPO−TDPA mixture—a coordinating solvent—CdTe nanocrystals could grow to elongated ones.[3]

If phosphonic acids were replaced by fatty acids, such as oleic acid (OA), the shape of the nanocrystals was varied between dots, rods, and tetrapods with a great purity as shown in Figure 2 (left panel) if a desired type of phosphine was used for dissolving the Te powder. The combination of OA and tributylphosphine (TBP) or trihexylphosphine (THP) always yielded dot-shaped CdTe nanocrystals. When trioctylphosphine (TOP) was used, growth of elongated CdTe nanocrystals became feasible. In the latter case, high initial monomer concentrations yielded almost pure tetrapods (Figure 2, bottom left), nearly monodisperse rods (Figure 2, middle left) were synthesized at medium level initial monomer concentrations, and at low initial monomer concentrations, dots with low yield were the only products (data not shown).

The influence of the chain length of phosphines observed in the OA-related reactions (Figure 2, left) should be considered to be one of the best indications of the ligand effects on monomers in the shape control of nanocrystals because phosphine molecules and their

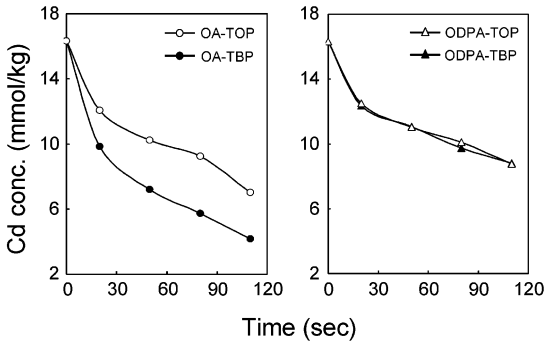

Figure 3. Temporal evolution of the remaining monomer concentration in the reaction solution.

possible derivatives were not found to be the ligands on the nanocrystals (see NMR and IR results below). This conclusion is further supported by the measurements described in the next paragraph and Figure 3.

The remaining cadmium concentrations of four representative reactions in Figure 2 (the ones with the same $[Cd]^0$) were determined and depicted in Figure 3 at given reaction times. The ODPA-to-Cd ratio and OA-to-Cd ratio were fixed as 2:1 and 4:1, respectively, which were approximately the lowest ligand-to-Cd ratios required to maintain a stable reaction system. The remaining monomer concentrations were always higher for the ODPA-related reactions in comparison to the OA-related reactions (Figure 3). The remaining monomer concentrations for both ODPA−TOP and ODPA−TBP were always identical within the experimental error.

However, in the OA-related cases, the remaining monomer concentrations were altered significantly by varying the chain length of the phosphines. It should be pointed out that the average number of CdTe units per nanocrystal in the first aliquots taken at about 20 s for the OA−TOP case (tetrapods) was significantly larger than that for the OA−TBP case (dots). A higher remaining monomer concentration and a larger sized crystal imply that the number of crystals existing in the OA−TOP reaction was less than that for the OA−TBP case. In other words, the number of nuclei formed in the OA−TOP system was much lower—approximately 10 times lower—than that in the OA−TBP case. Consequently, with use of TOP as the ligand for the Te monomer, the consumption of the monomers in the nucleation stage was significantly lower than that of the OA−TBP case.

Crystal Structure. The crystal structure of the CdTe nanocrystals formed with phosphonic acids or fatty acids, as the cadmium ligands are significantly different (Figure 4). The nanocrystals grown by the fatty acid-related reactions had a wurtzite structure, and the phosphonic acid-related reactions tended to yield nanocrystals with a zinc blende structure. Reaction temperature was an additional factor for determining the crystal structures. High reaction temperatures benefited the formation of wurtzite structure with less zinc blende stacking faults for the OA-related reactions, and nanocrystals with nearly perfect zinc blende structure were preferable at relatively low reaction temperatures for the ODPA-related reactions.

The similarity of wurtzite and zinc blende structures makes it difficult to judge the structure of a given sample without an appropriate simulation.[2] Figure 5

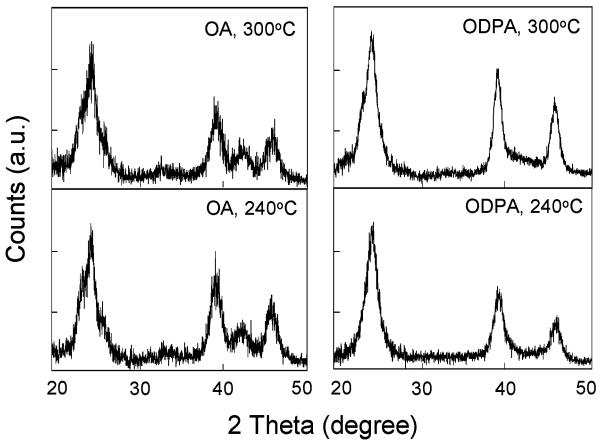

Figure 4. XRD patterns of CdTe dots formed with different ligands at different temperatures.

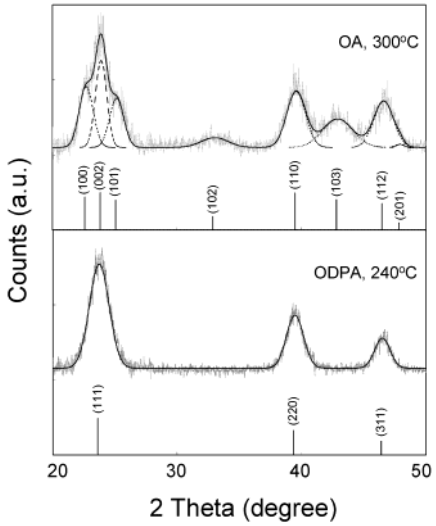

Figure 5. Simulation of XRD patterns (see text for details).

illustrates the peak fitting results for the two representative diffraction patterns, the 300 °C reaction using OA as the ligands (top left, Figure 4), and the 240 °C reaction using ODPA as the ligands (bottom right, Figure 4). The results revealed that the top pattern in Figure 5 fits well with a wurtzite structure with one stacking fault perpendicular to the *c*-axis. This single stacking fault significantly varied the diffraction pattern of the sample from a standard pattern. For example, the (103) diffraction peak is significantly broader than that of the adjacent (110) and (112) peaks, although the integrated area of (103) matches reasonably well the expected intensity.[2] The fitting of the bottom diffraction pattern in Figure 5 to a zinc blende structure was acceptable. The average crystal domain sizes calculated from the fitting parameters of all diffraction peaks were about 6.1 nm for the sample shown in the top plot of Figure 5 by assuming one stacking fault perpendicular to the (001) axis for this specific sample and 5.3 nm for the one shown in the bottom plot. The sizes of the nanocrystals determined by TEM were 5.8 nm for the wurtzite particle and 5.0 nm for the nanocrystals with zinc blende structure. The average sizes obtained from XRD and TEM matched each other reasonably well.

Overall Optical Properties, PL, and Absorption. The overall optical properties, PL, and absorption of the CdTe nanocrystals grown in the noncoordinating solvent

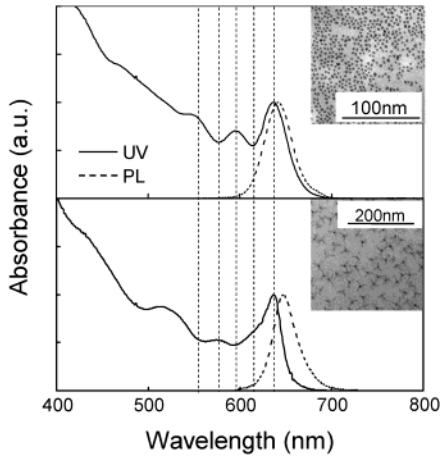

Figure 6. PL and UV−vis spectra of dots and elongated nanocrystals (tetrapods as an example).

are significantly better than those reported previously. The PL QY of CdTe nanocrystals synthesized using organometallic precursors reached about 50−70%, but the peak width was quite broad, with a fwhm of about 40−50 nm.[31,32] The PL of the CdTe nanocrystals synthesized in aqueous solutions also had a similar peak width.[33] The CdTe dots synthesized using alternative approaches in coordinating solvents can possess narrow emission lines, with a fwhm as narrow as 30 nm. However, the emission efficiency was only up to between 20% and 30%.[3]

PL QY of the CdTe dots synthesized through the schemes described here can reach as high as 70%. PL bright points observed in the growth of CdSe nanocrystals were also observed in this case.[11] Different from the CdSe nanocrystal system,[11,35] the difference in the maximum PL QY of CdTe nanocrystals coated with different ligands was insignificant. Although the crystal structures of the dot-shaped CdTe nanocrystals were found to be either zinc blende or wurtzite, a difference in optical properties between these two types of CdTe nanocrystals was not noticed. If multiple injections were involved, the PL QY of the samples was typically lower than the ones grown by a single injection. The PL QY of elongated nanocrystals was generally lower, 20−30% as the maximum. Although this is low in comparison with the values of the CdTe dots, it is at least comparable to the best values for CdSe rods, which were overcoated by CdS and ZnS shells.[36]

The difference in optical properties between semiconductor dots and elongated shapes has attracted significant attention recently.[37−40] Using existing elongated CdSe nanostructures, it is only possible to clearly identify the lowest absorption state because of the quality of the available samples. As shown in Figure 6, many absorption states can be clearly observed with the

(35) Kuno, M.; Lee, J. K.; Dabbousi, B. O.; Mikulec, F. V.; Bawendi, M. G. *J. Chem. Phys.* **1997**, *106*, 9869−9882.
(36) Manna, L.; Scher, E. C.; Li, L.-S.; Alivisatos, A. P. *J. Am. Chem. Soc.* **2002**, *124*, 7136−7145.
(37) Hu, J.; Li, L.-s.; Yang, W.; Manna, L.; Wang, L.-w.; Alivisatos, A. P. *Science* **2001**, *292*, 2060−2063.
(38) Li, L.-s.; Hu, J.; Yang, W.; Alivisatos, A. P. *Nano Lett.* **2001**, *1*, 349−351.
(39) Chen, X.; Nazzal, A.; Goorskey, D.; Xiao, M.; Peng, Z. A.; Peng, X. *Phys. Rev. B* **2001**, *64*, 245301−245304.
(40) Hu, J.; Wang, L.-w.; Li, L.-s.; Yang, W.; Alivisatos, A. P. *J. Phys. Chem. B* **2002**, *106*, 2447−2452.

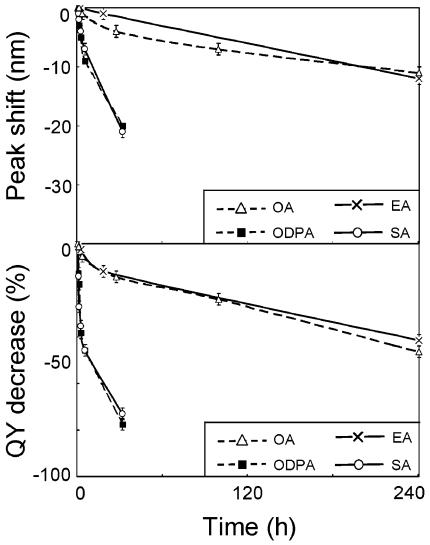

Figure 7. Oxidation of CdTe nanocrystals under ambient conditions.

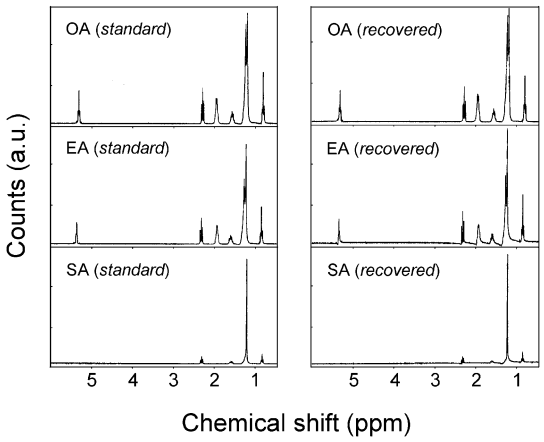

Figure 8. ^{1}H NMR spectra of the ligands recovered (right) and the standard ligands (left).

elongated CdTe nanocrystals. Evidently, although the dot and tetrapod samples in Figure 6 possess an identical position for the first absorption peak, the other absorption states of these two samples do not overlap at all. This indicates that the electronic energy structures of CdTe dots and elongated nanocrystals are completely different.

The as-prepared CdTe nanocrystals grown in ODE are only soluble in nonpolar organic solvents. They were successfully converted into water-soluble species by replacing the surface ligands with hydrophilic thiols using the established method.[41] The resulting water-soluble nanocrystals emitted surprisingly well. No deep trap emission was observed and no significant decrease in PL QY was observed. In contrast, highly luminescent CdSe nanocrystals coated with aliphatic amines became completely nonemitting by replacing the original surface ligands with hydrophilic thiols through the same protocol. Even for those CdSe/CdS and CdSe/ZnS core/shell nanocrystals, a significant PL QY decrease was often observed after the surface ligand replacement.[42,43] In this sense, CdTe nanocrystals may be a more promising system for biomedical applications using semiconductor nanocrystals.

Stability. The stability of the CdTe nanocrystals grown in ODE was found to be strongly dependent on the structure of the ligands on the surface of nanocrystals (Figure 7). Upon exposure to air, CdTe nanocrystals were gradually oxidized, indicated by the blue-shifted UV−vis and PL spectra. Simultaneously, those nanocrystals lost their PL (Figure 7). The oxidation of the highly luminescent CdTe nanocrystals, however, was suppressed by about two magnitudes using unsaturated fatty acids as ligands. In Figure 7, the three fatty acids and the phosphonic acid all possess a similar chain length, with 18 carbon atoms. Although the phosphonic acid, ODPA, bonds to the surface Cd atoms more strongly than the fatty acids do, the stability of the ODPA-coated nanocrystals was one of the two worst ones. CdTe nanocrystals coated with the saturated fatty acid—stearic acid—were oxidized at similar rates as the ones coated by ODPA.

^{1}H NMR Spectra. ^{1}H NMR spectra of the ligands recovered from the surface of CdTe nanocrystals synthesized using different fatty acids, OA, EA, or SA, are shown in Figure 8. In comparison to the standard spectra of free acids (left panel), one can conclude that the recovered ligands were only fatty acids, and no phosphines or their derivatives can be detected. The NMR signals at about 5.3 ppm, which are the ones for the hydrogen atoms of the −CH═CH− group in either OA or EA, did not show any significant change. These results clearly revealed that the unsaturated ligands on the surface of the nanocrystals were not polymerized. In addition, no structural change was observed for all three types of fatty acids on the surface of the nanocrystals.

FTIR Spectra. FTIR spectra of the CdTe nanocrystals coated with three different types of fatty acids are illustrated in Figure 9 (middle panel). For comparison, FTIR spectra of the free fatty acids (left panel) and the cadmium salts (right panel) are also shown in Figure 9. The results reveal that the ligands on the surface of the CdTe nanocrystals are the carboxylates, instead of free acids. The frequencies of the IR peaks related to $-COO^-$ groups in three cases are at the same positions, 1528 cm^{-1} for the asymmetric vibration and 1477 cm^{-1} for the symmetric vibration. This indicates that the interaction between the carboxylate groups and the surface cadmium ions is very similar in all three cases.

The small and almost evenly spaced peaks between 1180 and 1350 cm^{-1} have been identified as the fingerprints of the crystalline packed hydrocarbon chains in a zigzag configuration.[44−46] The small peaks are observed for EA, SA, $Cd(EA)_2$, and $Cd(SA)_2$ among the six control samples, indicating the crystalline packing of these four molecules. Oleic acid is liquid at room

(41) Aldana, J.; Wang, Y.; Peng, X. *J. Am. Chem. Soc.* **2001**, *123*, 8844−8850.
(42) Bruchez, M.; Moronne, M.; Gin, P.; Weiss, S.; Alivisatos, A. P. *Science* **1998**, *281*, 2013−2016.
(43) Guo, W.; Li, J. J.; Wang, Y. A.; Peng, X. *J. Am. Chem. Soc.* **2003**, *125*, 3901−3909.
(44) Bellamy, L. J. *The Infrared Spectra of Complex Molecules*, 3rd ed.; Halsted Press: New York, 1975.
(45) Peng, X.; Guang, S.; Chai, X.; Jiang, Y.; Li, T. *J. Phys. Chem.* **1992**, *96*, 3170−3174.
(46) Meulenberg, R. W.; Strouse, G. F. *J. Phys. Chem. B* **2001**, *105*, 7438−7445.

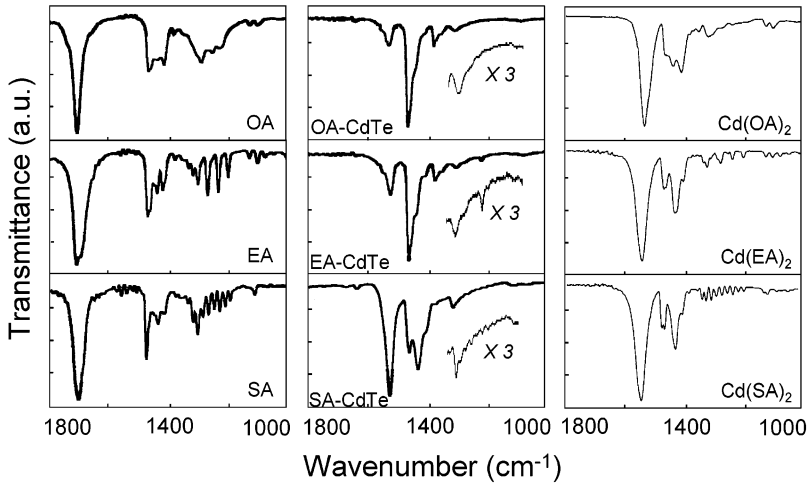

Figure 9. FTIR spectra. **Left**: free oleic acid (OA), elatic acid (EA), and stearic acid (SA). **Middle**: CdTe nanocrystals coated by the three types of fatty acids. **Right**: cadmium salts of the fatty acids.

temperature and such packing is impossible. Even with $Cd(OA)_2$, which is a waxy solid at room temperature, no zigzag packing of the hydrocarbon chain was observed. Among the nanocrystal samples, the zigzag packing was only observed in the case of the CdTe−SA sample. This indicates that the hydrocarbon chains of stearate ligands on the surface of a nanocrystal are at least partially packed in a zigzag configuration similar to that of crystalline long-chain paraffins. Similar zigzag packing was previously observed for CdSe nanocrystals coated with amine ligands with a saturated hydrocarbon chain.[46]

Discussion

The results shown above demonstrate several strong ligand effects on the nucleation, growth, and properties of CdTe nanocrystals. These ligand effects can be classified as two types, effects on monomers and effects on nanocrystals. The effects on the monomers should dominate ligand effects on the nucleation stage because nucleation is the process which creates the "seeds" for the growth/formation of crystals.

The bonding strength between ligands and cadmium ions significantly affected the nucleation process. When phosphonic acid was used, cadmium precursors were much less reactive in comparison to the cases with fatty acids. As a result, a small amount of monomers were consumed in the nucleation stage in general and formed a small amount of nuclei. This observation is consistent with other evidence. For example, if phosphonic acids were used as the ligands instead of fatty acids, nucleation of CdS and ZnSe nanocrystals was not possible under the same conditions reported in the previous work.[26] As mentioned above, to stabilize reactions with the same $[Cd]^0$, the concentration of fatty acids must be significantly higher in comparison to that of phosphonic acids. Phosphonic acids were so strong that the nucleation as well as the growth of the CdTe nanocrystals showed no response by varying the chain length of the phosphines that were used as the ligands for the Te monomers (Figure 3, right). In contrast, the nucleation process was dramatically affected by the chain length of the Te ligands, phosphines, when fatty acids were employed as the ligands for the cations. For the examples shown in Figure 3 (left panel), the number of nuclei was significantly less in the case of TOP than that when TBP was used (see related text in the Results section).

The ligand effects on monomers observed in the nucleation stage can be divided into three different classes. Class I, a strong coordination bond between monomers and ligands will decrease the reactivity of the monomers. Class II, ligands with longer hydrocarbon chains will suppress the reactivity of the monomers. Class III, as reported previously, the higher the ligand concentration is, the lower the reactivity of the monomers will be.[26,27] The last two effects are most likely due to steric factors and the first one is caused by the stability of the monomers. If the monomers are very stable, the steric effects will not play a role as demonstrated by the ODPA-related reactions (Figures 2 and 3). Overall, the nature, structure, and configuration of the ligands are important factors for determining the reactivity of the monomers. To take this into account, we should adopt monomer activity—"effective monomer concentration"—to replace the term monomer concentration currently used in the literature. The activity coefficient will cover both the steric and stability effects discussed here. Because temperature affects the stability and configuration of complexes, the activity coefficient should also be a function of reaction temperature. It would be important to experimentally determine or theoretically calculate the activity coefficient of monomers for different systems. For this work, we will limit ourselves to qualitative means.

If activity is considered, instead of monomer concentration, the shape difference shown in Figure 2 can be explained within the context of the existing model.[10,12] Due to their high chemical potentials, elongated shapes require a high chemical potential environment to grow.[10] This is equivalent to high monomer activity, which is a combination of a high remaining monomer concentration after nucleation and a high activity coefficient. However, to maintain a high remaining monomer concentration in solution for a sufficient period of reaction time, the concentration of nuclei must be low. If the nuclei concentration is too high, the high monomer concentration will quickly be depleted to an undesirable

low level due to the rapid consumption of monomers by the highly populated nuclei. Consequently, growth of elongated structures will no longer be supported. As discussed above, a low activity coefficient should suppress the number of nuclei in the solution.

In summary, for the formation of elongated shapes, the nucleation stage prefers a low activity coefficient and the growth stage requires a high activity coefficient. These two contradictory factors make a medium level activity coefficient a good choice for a simple reaction system. When phosphonic acids were used as ligands, the activity coefficient of cadmium monomers was too low to promote the growth of elongated shapes in noncoordinating solvents. If fatty acids and TBP were used, the activity coefficient of the monomers was too high and too many nuclei were formed (Figure 3); as a result, elongated shapes could not be formed. With fatty acids and TOP, elongated shapes could be formed at a relatively high initial monomer concentration due to a reasonable activity coefficient of the monomers.

Ligand effects on nanocrystals may be essential in helping the system break the inversion symmetry of the crystal structure, which is an intrinsic requirement for the growth of anisotropic nanocrystals. However, ligand effects on monomers seem to play a dominating role in the controlled growth of elongated CdTe nanocrystals, at least in the current system. As shown by NMR and IR studies (Figures 8 and 9), phosphines and their possible derivatives were not found to be the ligands of the resulting nanocrystals, although the chain length of the phosphines was the key in determining the shape of the nanocrystals in the OA-related reactions (Figure 2).

Although phosphonic acids prohibited the formation of elongated CdTe nanocrystals in ODE, it did promote the formation of elongated CdTe nanocrystals in a coordinating solvent, TDPA mixed with TOPO.[3] This can be simply explained by the decreased activity coefficient of the cadmium monomers by the excessive existence of a weak ligand, TOPO. The results observed in the formation of elongated CdSe nanocrystals in coordinating solvents suggested that the cadmium monomers at high temperatures should have both phosphonic acid and TOPO as their ligands.[10] Because these ligands are all somewhat labile at high temperatures, both types of ligands would have a chance to bond to cadmium atoms.

CdTe, CdSe, and CdS can all be in the form of either zinc blende or wurtzite structures. However, high-quality nanocrystals for both CdSe and CdS systems have been limited to the wurtzite form. Therefore, the control over the crystal structures of high-quality CdTe nanocrystals by varying the nature of the ligands in noncoordinating solvents (Figures 4 and 5) was somewhat surprising. For small nuclei, the theoretical results of Alivisatos's group[47] and our experimental results on CdSe nanocrystals[10] indicate that zinc blende should be the preferable structure. The formation of dot-shaped wurtzite CdSe and CdTe should be a result of a sudden phase transition when the size of the particles reaches a critical value.[10] This transition has also been observed in the case of CdS formed in aqueous solutions, from "magic-sized clusters" with zinc blende bonding geometry to largely sized CdS wurtzite nanocrystals.[48] In the existing literature, such a phase transition was considered to be possible when a significant supply of reactants existed in the reaction solution.[10] Because phosphonic acids strongly suppress the activity coefficient of cadmium monomers, such a transition could become difficult even at relatively high monomer concentrations. Consequently, the zinc blende structure of the nuclei is "arrested" and grows slowly to large-sized zinc blende nanocrystals. When the reaction temperature is lower, the decomposition of both Cd−phosphonate and Cd−carboxylate should become more difficult. As a result, lower temperatures should benefit the formation of zinc blende crystals for the phosphonic acid-related reactions and zinc blende stacking faults in the wurtzite nanocrystals for the fatty acid-related reactions.

The above explanation of the control of the crystal structures is solely based on ligand effects on monomers. There is an alternative interpretation of this interesting phenomenon. Phosphonic acids bond strongly to cadmium atoms on the surface of a nanocrystal in comparison to fatty acids. The phase transition of the nanocrystal could be hindered by these strong ligand−nanocrystal interactions. However, this alternative explanation is not consistent with the results observed in the reactions performed in coordinating solvents. When CdTe nanocrystals were synthesized in a coordinating solvent,[3] TOPO mixed with TDPA, the nanocrystals were wurtzite, although NMR studies confirmed that TDPA were the only ligands on the surface of the nanocrystals. In the context of ligand effects on monomers, the formation of wurtzite structure in the coordinating solvents can be explained by the enhanced activity coefficient of cadmium monomers due to the excessive existence of a weak ligand (TOPO) as discussed above.

Evidence has revealed that the stability of zinc blende nanocrystals at high temperatures increases as the atomic mass of anions of the cadmium chalcogenides increases.[22] This is probably the intrinsic reason the control of crystal structures of high-quality CdTe nanocrystals is the first to be realized. The high-temperature stability of the zinc blende structure of CdTe nanocrystals can also explain why it is much easier to form tetrapods with a very high yield (Figures 2 and 6). It was previously reported that the center of the tetrapods is a zinc blende core,[10,20] which provides four (111) facets for the growth of four wurtzite arms elongated along their (001) axis.

Oleic acid has been noticed as a special ligand that can yield much more stable active metal nanocrystals than other saturated fatty acids.[19] The evidence described in the Results section revealed that such stability is provided by the random packing of the hydrocarbon chain of the ligand monolayer (Figures 8 and 9). In the case of stearic acid, a saturated fatty acid, the hydrocarbon chains are packed in a crystalline manner, at least partially. Such crystalline packing of the hydrocarbon chains of the ligands on a nanocrystal creates gaps between each crystalline domain, provided

(47) Alivisatos, A. P. MRS Spring Meeting, 2003.

(48) Vossmeyer, T.; Katsikas, L.; Giersig, M.; Popovic, I. G.; Diesner, K.; Chemseddine, A.; Eychmuller, A.; Weller, H. *J. Phys. Chem.* **1994**, *98*, 7665−7673.

the spherical nature of the nanocrystal surfaces. These gaps act as the diffusion channels for oxygen molecules. Consequently, this makes the nanocrystals significantly less stable if they are coated with ligands with a saturated hydrocarbon chain. This phenomenon is similar to the enhanced stability of nanocrystals by coating them with hype-branched ligands, organic dendron ligands.[49]

(49) Wang, Y. A.; Li, J. J.; Chen, H.; Peng, X. *J. Am. Chem. Soc.* **2002**, *124*, 2293−2298.

Acknowledgment. The financial support of this work is provided by the National Science Foundation and the University of Arkansas.

Supporting Information Available: Figure depicting size-dependent absorption peak position, details of the multiple-injection experiment, and TEM images of differently sized dots and tetrapods (PDF). This material is available free of charge via the Internet at http://pubs.acs.org.

CM034729T